Sliding behavior monitoring of a deep seated landslide with differential interferometric synthetic aperture radar, mems tiltmeter and unmanned vehicle images

K.-L. Wang[a], Y.-M. Hsieh[b], J.-T. Lin[a] and M.-H. Hsi[a]

[a]Department of Civil Engineering, Nationl Chi Nan University, Taiwan
[b]Department of Construction Engineering, National Taiwan University of Science and Technology, Taiwan
E-mail: klwang@ncnu.edu.tw, ymhsieh@mail.ntust.edu.tw, nokilin@gmail.com, ilovevachen@gmail.com

Abstract

Landslide is a common issue in Taiwan with more than 70% area of this island is mountainous land. Typhoons and earthquakes attack Taiwan every year even by month. People lost their lives, properties and wounded when landslides happened during typhoons, heavy rainfall and earthquake. Landslide hazard mitigation is very important in hazard prevention chain. Two deep-seated landslides selected for monitoring in this research. A visual approach calls red relief image is applied in the beginning to search scars, geological structure on the ground surface. Synthetic aperture radar images acquired by JAXA (Japan) are used in this research to monitor landslide displacement in large area. The electromagnetic waves from temporal images can use to derive differential between time period. Thus the displacement can be coverted from phase differences. Mems monitoring stations are set up after differential interferometric results. The memes sensors are cost effective to monitoring landslide tilt behavior 24 hours. Moreover, unmanned vehicle system is adopted in this research to see optical differences on ground surface. The results show good coincidence with each other monitoring methods.

Keywords –

Landslide; SAR; Mems; UAS

1 Introduction

Taiwan locates in the collision zone of sea plate and continental plate, which inducing earthquake and orogeny. Moreover, this island is surrounded with warm and cool sea water. Typhoons and heavy rainfall attacked this island frequently, especially after year 2000. Several typhoons and heavy rainfall with unexpected large rainfall attacked Taiwan in past 10 years. Typhoon Morakot in 2009 brings maximum 3,000 mm accumulated rainfall and the rainfall is 3/4 of average annual precipitation.

Landslide potential map is the first work for landslide hazard mitigation. There are several methods to produce landslide potential map. The logistic regression method combines potential factors with landslides and give landslide potential prediction. Two major categories including bivariate analysis and multivariate analysis are used in logistic regression analysis. Gupta and Joshi (1990) used Landslide Nominal Risk Factor (LNRF) to derive dimensionless factors and calculate the potential risk. Jade and Sarkar (1993) adopted Information Theory and classified the potential risk into three classes. Keefer (2000) proposed a landslide concentration (LC) factor to establish the relationship between landslide and earthquake. The landslide susceptibility mapping using bivariate analysis without seismic condition was conducted by different researchers. (Çevik et al., 2003; Chau et al., 2004; Lee, 2004; Lee et al., 2004; Lee, 2005; Ohlmacher and Davis, 2003). However, the bivariate analysis does not take into account the independency of factors. Therefore, multivariate analysis has been developed for that purpose. The independency of factors must be checked and the matrix of factors is thus established. Two classification algorithms – logistic regression and discriminating analysis are the most well-known methods to identify the susceptibility of landslide. Lin and Tung (2004) used structural equation model to establish a measuring matrix for landslide evaluation for the cases of Chi-Chi earthquake. Süzen and Doyuran (2004) compared the landslide susceptibilities using bivariate and multivariate analysis (logistic regression) based on northwest Turkey study area.

The neural network analysis uses factors related to landslides to perform training and evaluation of landslide susceptibility. The accuracy can be as high as 90% in the same area and using same event (Lee et al., 2003). However, the training process needs to restart when encountering different condition.

Semi-logistic regression methods which combined factor of safety to produce probability of landslide can be used to establish the susceptibility map. Pack et al. (1998, 1998a, 2001) used the stability index derived from factor of safety to classify susceptibility into several groups: stable, moderately stable, quasi-stable, lower threshold, upper threshold, and defended. Lan et al. (2004) used the module to analyze the landslide hazard in Yunnan, China. Another semi-logistic method adopts displacement as the index of landslide susceptibility. Wang et al. (2010) proposed a semi-mechanical and semi-regression method to produce landslide potential map.

The study is trying to propose a method to produce landslide potential map from differential interferometric synthetic aperture radar (DInSAR). Potential landslide zones are mapped after fringes and displacements are generated from ALOS/PALSAR radar image processing. Meanwhile, a deep-seated landslide site has been selected for instrumentation. Monitoring data from Mems has been collected and analyzed to find relationship between landslide displacement and rainfall, and groundwater. Mems accelerometer is designed for active or quick displacement area. The design is considered tilt and dynamic data collection. Moreover, unmanned vehicle system is adopted to produce high resolution, high precision digital elevation to compare previous results.

2 Methodology

The study area is located at central Taiwan and the elevation ranges from 1000m to 2500m. A landslide potential map was mapped by expert from LiDAR data, which means the scars were generated by some events with unknown years and unknown active status. The scars in study area are as shown in Figure 1. Most aspects of scars are facing north or south-north owing to geological condition. The geological condition in this area is quite unique, which is slate of Lushan Formation, Miocene. Lushan Formation is slate interlayered with thin metamorphosed sandstone and slate. The dip angles of slate in this area ranges from 20-70 degrees owing to gravity and tectonic forces.

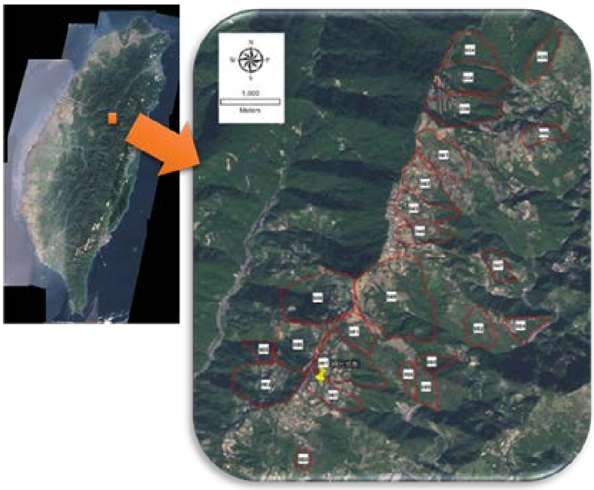

Figure 1 Landslide mapping with LiDAR data in study area.

2.1 Benchmark survey

Benchmark survey was executed by local government from plain area to mountain area. The differences in elevation is as shown in Figure 2 The differences are almost increasing except some benchmarks. The increasing of elevation is undoubtedly the effect orogeny. If rank the elevation difference and select a threshold for stable zone, the others can be eliminated the average value of stable zone. The benchmarks locate in landslide scars can be identified and the true landslide displacement can be calculated based on this assumption as shown in Figure 3. There are four benchmarks show elevation decreasing, which means locate in landslide scar and moving between 2002~2008. The displacement has been calculated as shown in Tab. 1. The values have been transferred to annual velocity for DinSAR comparison.

Figure 2 The elevation change from benchmark survey in 8 years (2002-2009)

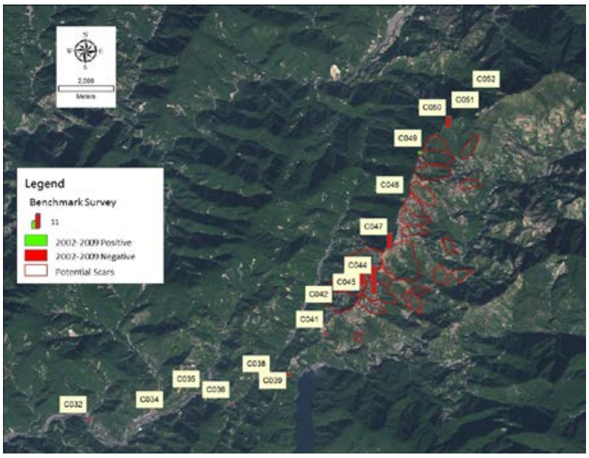

Figure 3 Elevation differences adjusted for landslide displacement

Table 1 Elevation differences derived for landslide velocity

Landslide Number	Relative decreasing velocity (mm/year)
C050	8.02
C047	12.03
C045	9.90
C044	22.06

2.2 Potential landslide mapping with DInSAR

SAR measures the distance between satellite and ground surface by sending and receiving radar signals. Measurement of ground topography using SAR represents two locations of antenna that sensing the surface and are separated by a baseline. If the viewing geometry is controllable or known with sufficient accuracy, then the topography h can be derived from the phase measurement of the two sensing radar waves. The topography h can be obtained by geometry of satellite and observation point. Two important conditions that need to be understood for detecting and measuring surface change with SAR are:

(1) The changes between two successive images must not be too large.

(2) The radar-scattering characteristics within each pixel must remain similar.

The deformation of ground surface derived from DInSAR could be less than centimeter with high accuracy digital elevation model. When doing interferometry analysis by temporal SAR data, the phase information generated is including topography, change of ground characteristics, ground movement and atmosphere effect, etc. (eq.1) Phase difference of topography can be removed by high accuracy digital elevation model and short base line. Atmosphere effect can be reduced by long term analysis. The deformation can be trusted to high precision and after removed previous described errors and simply left ground deformation and noise.

$$\emptyset_{Int} = 4\pi\frac{R_1 - R_2}{\lambda} = \Phi_{Topography} + \Phi_{Change} + \Phi_{Movement} + \Phi_{Atmosphere}$$

$$= \frac{4\pi B_n}{\lambda R \sin\theta} h + \Phi_{change} + \frac{4\pi}{\lambda}\Delta R_{Movement} + \Phi_{Atmosphere}$$

$$= \frac{4\pi B_n}{\lambda R \sin\theta} h + \frac{4\pi}{\lambda}\Delta R_{Movement} + \Phi_{Noise} \qquad [1]$$

in which,
R: distance from satellite to observation position
B: Baseline length
h: elevation
λ: wave length of radar
θ: side looking angle

DInSAR, PS, and SBAS has been well developed in recent years thus the monitoring of landslide displacement is becoming more possible. (Pieraccini, Casagli et al. 2003, Tarchi, Casagli et al. 2003, Guzzetti, Manunta et al. 2009, Cal, x00F et al. 2013, Liu, Wang et al. 2013, Lowry, Gomez et al. 2013, Jebur, Pradhan et al. 2015, Tang, Chen et al. 2015, Casagli, Cigna et al. 2016, Uhlemann, Smith et al. 2016)

The SAR images used in this research is Advanced Land Observing Satellite (ALOS) Phased Array type L-band Synthetic Aperture Radar (PALSAR) L band image. The polarization of radar electromagnetic wave is Horizontal - Horizontal (HH) mode and incident angle is 34.3 degree. The range resolution from this area is approximately 10 meter. There are several SAR images can be used for differential interferometric SAR. However, ALOS PALSAR with L band has longer wave length, which is 23cm and possible could be eliminated the effect of vegetation.

The results of no significant rainfall event and typhoon event are as shown in Figure 4 and Figure 5, separately. Nine large landslide scars were mapped comparing with event and no event data. Comparing with Figure 4 and Figure 5, there are some higher displacement points located in the middle of slope. This might be due to landslide moving and the scar comes out from middle of slope.

DInSAR method is fine to observe landslide scar at two images with close dates. However, the displacement data shows too much noise to identify accuracy and comparison with benchmark data. Thus another approach small baseline subset (SBAS) is adopted for higher accuracy. This method searches points with the same radar signal strength through observing years and keep tracking locations in each scene. Figure 6 shows the result of SBAS method with larger zone of study area. The RMS error directly from radar shows 10mm with 95% confidence.

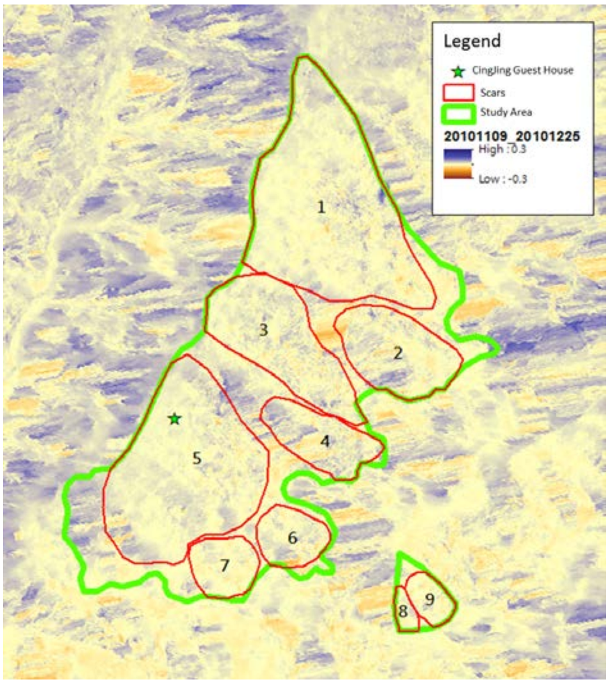

Figure 4 The displacement generated by DInSAR from multi-temporal data (2006-2010; no events)

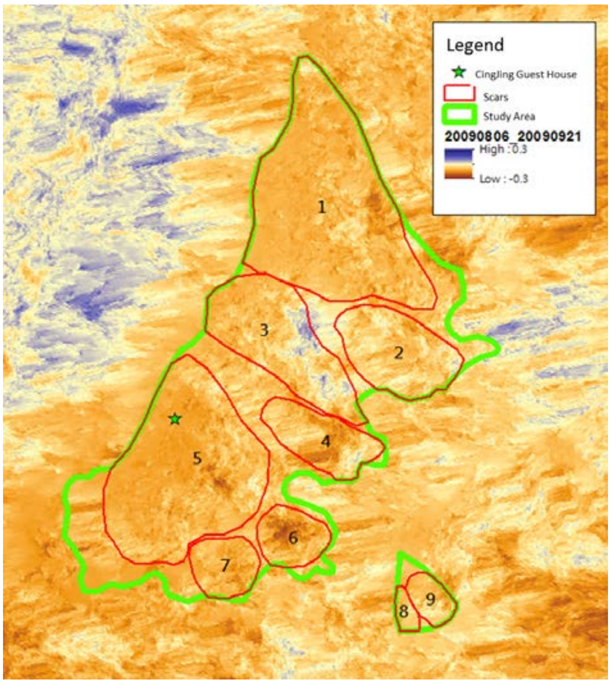

Figure 5 The displacement generated by DInSAR from multi-temporal data (2006-2010; typhoon event)

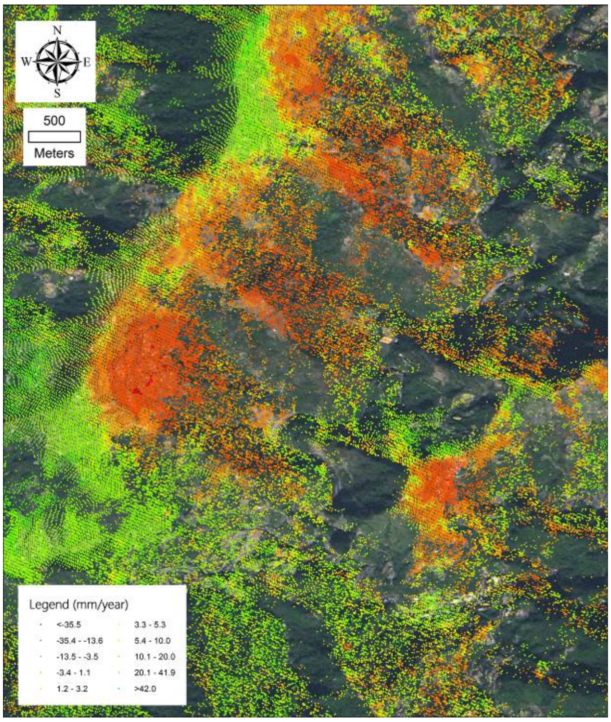

Figure 6 Displacement velocity map produced with SBAS from 2006-2016

2.3 Mems instrumentation

Owing to the area of slide number 8 and 9 in Fig. 4 is about 34 hectares, total landslide instrumentation is too expensive and unnecessary. In this work, we present a low-cost slope-monitoring device. The device is constructed using components purchased online at reasonable costs. The device is capable of recording triaxial accelerations at 200Hz onto standard SD (secure digital) memory cards. In addition, the sensed triaxial accelerations can be converted to tilt, which can then be sent via onboard GPRS module to a cloud server. Thus, the constructed device can be used for both static measurements of the slope surface and dynamic measurements of ground-surface acceleration. This information can assist assess slope condition regularly and dynamic force experienced by the slope after earthquake. The recorded data has been transferred into tilt as shown in Figure 7.

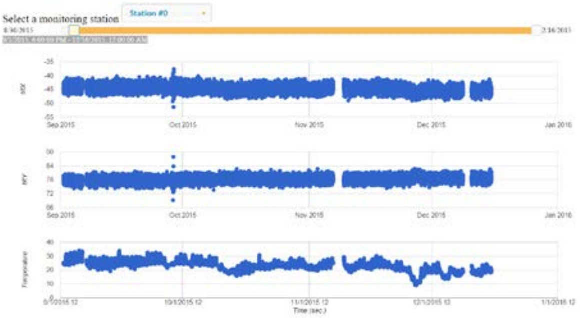

Figure 7 Tilt measurement data within three months

2.4 Unmanned vechicle system

Field investigation is time consuming, high budget, limited data collected and dangerous. Investigation with satellite images has disadvantages such as less of the actual situation and poor resolution. Thus the possibility for slope investigation with UAV will be proposed and discussed in this research. Hazard investigation and monitoring is adopted UAV in recent years. UAV has advantages such as light weight, small volume, high mobility, safe, easy maintenance and low cost. Investigation can be executed in high risk area. Use the mature aero photogrammetry , combines aero photos with control point. Digital surface model (DSM) and Ortho photos can be produced with control points aligned. The resolution can be less than 5cm thus can be used as temporal creeping monitoring before landslide happens. Figure 8 shows the red relief image map from UAS result. The scars can be identified from that and have nice coincidence with previous results.

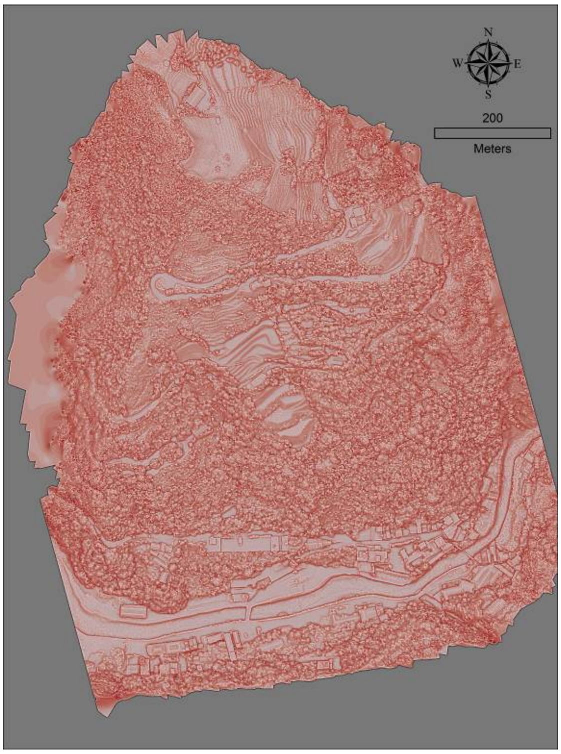

Figure 8 Red relief image map produce from UAS result

3 Conclusions

Landslide potential map is typically generated by factors by statistic method or mechanic equilibrium approach. In this work we propose a monitoring methodology from DInSAR and SBAS data processing. This method can identify active landslide scars in the same rainfall condition area, which means should pay more attention to monitoring. DInSAR can map landside scars from fringe and displacement map. The SBAS has more precise displacement monitoring with linear modeling.

A deep seated landslide was selected for instrumentation to compare with DInSAR and SBAS method.

The underground instrumentations show that landslide displacement has good coincidence with accumulative rainfall. However, landslide instrumentation is too expensive when there are many potential scars in study area. Thus a low-cost mems monitoring sensor was developed in this work. In this work, we share our experience on building a low-cost slope-monitoring device that senses temperature and dynamic accelerations at 200Hz, provides 6-month long-term storage with a 16GB micro SD card, and sends calculated tilt to cloud servers via GPRS module. The low-cost system works well and provides more quick response to landslide warning much earlier than DInSAR and SBAS methods.

References

[1] Cal, F., F. Ardizzone, R. Castaldo, P. Lollino, P. Tizzani, F. Guzzetti, R. Lanari and M. Manunta (2013) Landslide analysis through the multi-sensor SBAS-DInSAR approach: The case study of Assisi, Central Italy. 2013 IEEE International Geoscience and Remote Sensing Symposium - IGARSS. 2916-2919

[2] Casagli, N., F. Cigna, S. Bianchini, D. Hölbling, P. Füreder, G. Righini, S. Del Conte, B. Friedl, S. Schneiderbauer, C. Iasio, J. Vlcko, V. Greif, H. Proske, K. Granica, S. Falco, S. Lozzi, O. Mora, A. Arnaud, F. Novali and M. Bianchi (2016) Landslide mapping and monitoring by using radar and optical remote sensing: Examples from the EC-FP7 project SAFER. Remote Sensing Applications: Society and Environment 4: 92-108.

[3] Chau, K.T., Y.L. Sze, M.K. Fung, W.Y. Wong, E.L. Fong and L.C.P. Chan (2004) Landslide hazard analysis for Hong Kong using landslide inventory and GIS. Computers and Geosciences. 30:429-443

[4] Gupta, R.P and B.C. Joshi (1990) Landslide Hazard Zoning Using the GIS Approach – A Case Study from the Ramganga Catchment, Himalayas. Engineering Geology. 28:119-131

[5] Guzzetti, F., M. Manunta, F. Ardizzone, A. Pepe, M. Cardinali, G. Zeni, P. Reichenbach and R. Lanari (2009). Analysis of Ground Deformation Detected Using the SBAS-DInSAR Technique in Umbria, Central Italy. Pure and Applied Geophysics. 166(8): 1425-1459.

[6] Jade S. and S. Sarkar (1993) Statistical models for slope instability classification. Engineering Geology., 36:91-98

[7] Jebur, M. N., B. Pradhan and M. S. Tehrany (2015) Using ALOS PALSAR derived high-resolution DInSAR to detect slow-moving landslides in tropical forest: Cameron Highlands, Malaysia. Geomatics, Natural Hazards and Risk 6(8): 741-759.

[8] Keefer D.K. (2000) Statistical analysis of an earthquake-induced landslide distribution – the 1989 Loma Prieta, California event. Engineering Geology. 58:231-249

[9] Lan H.X., C.H. Zhou, L.J. Wang, H.Y. Zhang and R.H. Li (2004) Landslide hazard spatial analysis and prediction using GIS in the Xiaojiang watershed, Yunan, China. Engineering Geology. 76:109-128

[10] Lee, C. N. (2001) Preliminary study on the Tsao-Ling landslide area under earthquake. Master’s Thesis. National Taiwan University

[11] Lee S. (2004) Application of likelihood ratio and logistic regression models to landslide susceptibility mapping using GIS. Environmental Management. 34(2):223-232

[12] Lee S. (2005) Application of logistic regression model and its validation for landslide susceptibility mapping using GIS and remote sensing data. International Journal of Remote Sensing. 26(7):1477-1491

[13] Lin, M. L. and C.C. Tung (2004), A GIS-based potential analysis of the landslides induced by the Chi-Chi earthquake. Engineering Geology. 71:63-77

[14] Liu, G., R. Wang, Y. K. Deng, R. Chen, Y. Shao, W. Xu and D. Xiao (2013). Monitoring of ground deformation in Beijing using SBAS-DInSAR technique. 2013 Asia-Pacific Conference on Synthetic Aperture Radar (APSAR). 300-303

[15] Lowry, B., F. Gomez, W. Zhou, M. A. Mooney, B. Held and J. Grasmick (2013) High resolution displacement monitoring of a slow velocity landslide using ground based radar interferometry. Engineering Geology. 166: 160-169.

[16] Ohlmacher G. C. and J.C. Davis (2003) Using multiple logistic regression and GIS technology to predict landslide hazard in northeast Kansas, USA. Engineering Geology. 69:331-343

[17] Pack, R. T., D.G. Tarboton and C. N. Goodwin (1998) The SINMAP approach to terrain stability mapping. The 8th Congress of the International Association of Engineering Geology, Vancouver, Canada

[18] Pack, R. T., D.G. Tarboton and C.N. Goodwin (1998a) Terrain stability mapping with SINMAP, technical description and user guide for version 1.00. Report Number 4114-0, Terratech Consulting Ltd., Salmon Arm, B.C., Canada

[19] Pack, R. T., D.G. Tarboton and C.N. Goodwin (2001) Assessing terrain stability in a GIS using SINMAP. The 15th annual GIS conference, Vancouver, Canada

[20] Pieraccini, M., N. Casagli, G. Luzi, D. Tarchi, D. Mecatti, L. Noferini and C. Atzeni (2003) Landslide monitoring by ground-based radar interferometry: A field test in Valdarno (Italy). International Journal of Remote Sensing. 24(6): 1385-1391.

[21] Süzen, M.L. and V. Doyuran (2004) A comparison of the GIS based landslide susceptibility assessment methods: multivariate versus bivariate. Environmental Geology. 45:665-679

[22] Tang, P., F. Chen, H. Guo, B. Tian, X. Wang and

N. Ishwaran (2015) Large-Area Landslides Monitoring Using Advanced Multi-Temporal InSAR Technique over the Giant Panda Habitat, Sichuan, China. Remote Sensing. 7(7): 8925.

[23] Tarchi, D., N. Casagli, S. Moretti, D. Leva and A. J. Sieber (2003) Monitoring landslide displacements by using ground-based synthetic aperture radar interferometry: Application to the Ruinon landslide in the Italian Alps. Journal of Geophysical Research: Solid Earth. 108(B8): n/a-n/a.

[24] Uhlemann, S., A. Smith, J. Chambers, N. Dixon, T. Dijkstra, E. Haslam, P. Meldrum, A. Merritt, D. Gunn and J. Mackay (2016) Assessment of ground-based monitoring techniques applied to landslide investigations. Geomorphology. 253: 438-451.

[25] Wang, K.-L. and M.-L. Lin (2010) Development of Shallow Seismic Landslide Potential Map Based on Newmark's Displacement: The Case Study of Chi-Chi Earthquake, Taiwan. Environmental Earth Sciences. 60(4), 775-785